

Highly Efficient Resonant Wireless Power Transfer with Active MEMS Impedance Matching

Bernard Ryan
Solace Power
Mount Pearl, NL, Canada
bernard.ryan@solace.ca

Marten Seth
Menlo Microsystems
Irvine, CA, USA
marten.seth@menlomicro.com

Christopher Rouse
Solace Power
Mount Pearl, NL, Canada
chris.rouse@solace.ca

Christopher Kennedy
Solace Power
Mount Pearl, NL, Canada
chris.kennedy@solace.ca

Christopher Giovanniello
Menlo Microsystems
Irvine, CA, USA
chris.giovanniello@menlomicro.com

Abstract—This work presents a new method of dynamic impedance matching for use in fixed-frequency resonant wireless power transfer (WPT) systems. In particular, a six channel Micro-Electromechanical System (MEMS) based switch is used to obtain variable shunt capacitance in a double-L matching network topology. A brief overview of the MEMS switch is provided and attention is then focused on its use in the context of resonant capacitive coupling WPT systems operating at 13.56 MHz and 27.12 MHz. Consideration of the MEMS switch voltage and current handling capabilities then leads to practical design limits. Measurements are carried out at a power level of 75 W and WPT impedance matching is demonstrated over a resonator displacement range of 100 mm – 200 mm. The performance of the proposed MEMS based double-L matching network is then compared against modelled results and analyzed in terms of matchable impedance range, impedance match accuracy, node voltages, and efficiency.

I. INTRODUCTION

Resonant wireless power transfer (WPT) systems can present very large impedance variations to the system's transmitter (Tx) power electronics [1]. These impedance variations may occur as the result of relative movement between the receiver (Rx) and Tx, environmental changes such as the presence of foreign objects, or from changes in Rx loading. In order to source adequate radio frequency (RF) power from the Tx power amplifier or inverter the impedance presented must be controlled. One method of maintaining a constant source loading is to use frequency tracking, which follows one of the resonant frequency peaks. However, frequency spectrum regulations largely prohibit this broadband technique. An alternative method, is to use a narrowband dynamic impedance matching network to transform the changing wireless link impedance to a desired target impedance.

This work presents an impedance matching circuit which uses Micro-Electromechanical System (MEMS) based switch components to improve the operation of a WPT system. In particular, the MM3100, a six channel MEMS switch, is used to

obtain variable capacitance by switching fixed value shunt capacitors in and out of circuit in a double-L matching network. The MEMS-based chip shown in Fig. 1 is an attractive option for WPT impedance matching because it provides a way to vary capacitance with minimal effect on insertion loss, while withstanding the high voltages that arise in resonant WPT. These features facilitate efficient impedance matching at high transmit power levels.

This paper briefly describes MEMS and their unique benefits in the application of WPT impedance matching. In particular, WPT impedance matching with MEMS technology is demonstrated at a transmit power level of 75 W for the industrial, scientific and medical (ISM) band frequencies of 13.56 MHz and 27.12 MHz. To highlight the large impedance swings which occur in resonant WPT systems, typical impedances of a resonant capacitive coupling (RCC) WPT system are presented. The voltage and current limits of the MM3100 are then used to obtain practical constraints on the range of matchable impedances and transmit power level. Assuming a transmitted power level of 75 W, a comparison of modelled and experimental results is undertaken considering the match accuracy, branch voltages, and efficiency of the matching network.

II. MICRO-ELECTROMECHANICAL SYSTEM SWITCH DEVICES

Recent advances in processing capability and metallurgy have enabled new kinds of MEMS devices that combine the on-state conductivity of metal contacts with stable mechanical properties that enable both long and reliable operation and temperature stability. The electrical properties are very similar

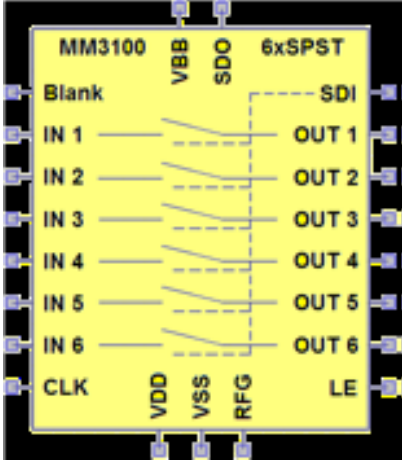


Fig. 1. MM3100 MEMS-based six channel switch schematic.

to electromechanical relays with orders of magnitude better reliability, faster switching speed ($< 10 \mu\text{s}$), and a more attractive form factor, similar to that of a semiconductor device. An example of this technology can be found in [2]. Compared to the commonly used PIN diode [3], the MEMS-based switch offers low insertion loss (on resistance $< 0.5 \Omega$), excellent consistency, and the ability to withstand voltages of several hundred volts. Further, the use of electrostatic control of the MEMS switch enables additional energy savings in the control and bias circuitry with no current drain in a steady state hold operation. The MM3100 also features a digital SPI interface for controlling the six switches.

III. WIRELESS POWER IMPEDANCE MATCHING WITH THE MM3100

The double-L matching network topology considered in this paper is shown in Fig. 2. It consists of two fixed series inductors, L_1 and L_2 , two fixed shunt offset capacitors, C_{O1} and C_{O2} , and two variable shunt capacitor branches, C_{V1} and C_{V2} . Each of these variable capacitor branches consists of six parallel capacitors which are switched in and out of circuit using a single MM3100. The load impedance, Z_L , is the impedance presented to the network by the wireless link. Fig. 3 shows how this impedance changes as a function of resonator separation for a typical RCC WPT system. This data was obtained using CST Studio Suite electromagnetic simulation software for operating frequencies of 13.56 MHz and 27.12 MHz. As conveyed in the Fig. 3, the impedances to be matched can range from tens of ohms into the thousands of ohms. If operation over the entire range is desired, the matching network must be able to transform these load impedances to some target impedance, Z_0 . As such, the main objective of the matching network is to make the transformed impedance Z_{in} as close to Z_0 as possible.

With an aim of maximizing the range of load impedances the double-L network can match, it is desirable to maximize the amount of variable capacitance C_{V1} and C_{V2} . The per branch voltage and current ratings of the MM3100 place a theoretical limit on the maximum branch capacitance that can be used. Here the maximum capacitance is calculated for the worse-case scenario of maximum current and voltage occurring at the same

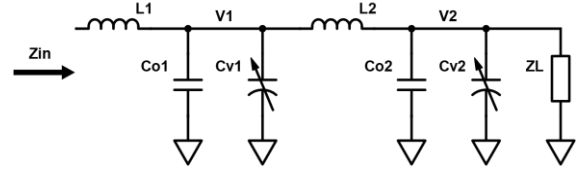


Fig. 2. Double-L Matching Network with MEMS Variable Capacitor Branches.

time. In general, the maximum branch capacitance, C_{max} , is given by the following expression,

$$C_{max} = \frac{I_{max}}{\omega V_{max}} \quad (1)$$

where ω is the radian operating frequency and I_{max} , V_{max} are the maximum branch current and maximum branch voltage, respectively. For the MM3100, $I_{max} = 1 \text{ A}_{\text{rms}}$ and $V_{max} = 141 \text{ V}_{\text{rms}}$. Inserting these values into equation (1) gives $C_{max} = 83 \text{ pF}$ for 13.56 MHz and $C_{max} = 41.5 \text{ pF}$ for 27.12 MHz. In theory, every branch could use these values, but in practice more resolution is necessary to obtain reasonable matching performance over a broad range of load impedances. In practice, step sizes of 10 pF at 13.56 MHz and 5 pF at 27.12 MHz are sufficient to ensure good performance. For the 13.56 MHz case the six capacitor branches are specified as 10, 20, 40, 80, 80, and 80 pF, giving a maximum variable capacitance of 310 pF with a step size of 10 pF for both C_{V1} and C_{V2} . For 27.12 MHz these values are all halved.

A. Maximum Transmitted Power Limitations

The voltage rating of any switching component places constraints on either the maximum impedance and/or maximum transmitted RF power level an impedance matching circuit can handle. Considering only real load impedances, $Z_L = R_L$, the maximum power that can be delivered is given by,

$$P_{max} = \frac{V_{max}^2}{R_L} \quad (2)$$

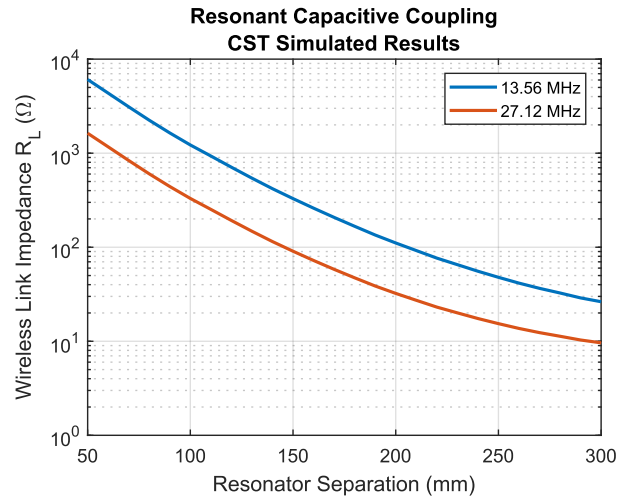


Fig. 3. Wireless Link Impedances, R_L , for an example Resonant Capacitive Coupling WPT System.

If power is increased beyond P_{max} the voltage limit of the switch on the C_{V2} branch will be exceeded. In the case of the MM3100, it is critical not to significantly exceed this voltage as it can lead to a self-actuated hot-switch event that may be harmful to the device. There is a clear trade-off between the amount of power that can be transmitted and the maximum impedance that loads the matching network. Setting a transmitted power level thus places a limit on the matchable range. In the case of a transmitted power level of 75 W and recalling that for the MM3100 $V_{max} = 141 V_{rms}$, the maximum load impedance is given by $R_{L_{max}} = 265 \Omega$. It is possible to operate at higher load impedances, but the input power must then be decreased in accordance with Equation (2).

B. Range of Matchable Impedances

In addition to being able to handle the voltage at rated power, the matching network must also be capable of transforming the range of load impedances to the target source impedance. This network must use the range of variable capacitance previously determined. Fig. 4 shows the matchable range of impedances on a Smith chart in blue for one such network. The operating frequency is 13.56 MHz and the target source impedance, Z_0 , is 50 Ω . The maximum impedance, $R_{L_{max}} = 265 \Omega$, is indicated by a red X. This network has the added benefit of being able to tune out extra load reactance. Resonator detuning, environmental changes, or transmission line length can lead to non-real load impedances, so the ability to properly match non-real impedances is highly desirable.

Fig. 5 shows a similar matchable range of impedances for a system operating at 27.12 MHz. It should be noted that both the capacitor and inductor values are approximately half of the values used for the 13.56 MHz matching network of Fig. 4. These values were chosen intentionally to keep the total amount of reactance the same for both matching networks. This is reflected in the fact the similar portions of the Smith chart can be matched for both networks.

Smith Chart of Matchable Impedances (f = 13.56 MHz)

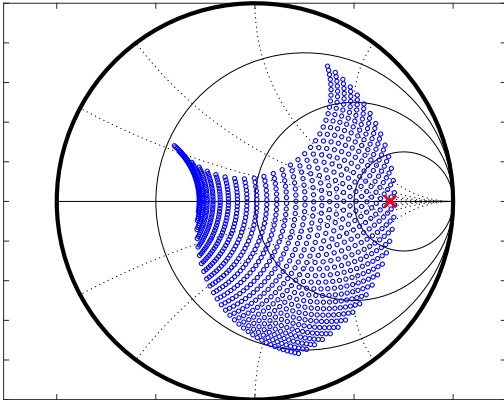


Fig. 4. Impedances matchable to $Z_{in} = 50 \Omega$. (Frequency = 13.56 MHz, $L_1 = 680 \text{ nH}$, $L_2 = 680 \text{ nH}$, $C_{01} = 310 \text{ pF}$, $C_{02} = 156 \text{ pF}$, Inductor $Q_1 = 350$, $Q_2 = 350$).

Smith Chart of Matchable Impedances (f = 27.12 MHz)

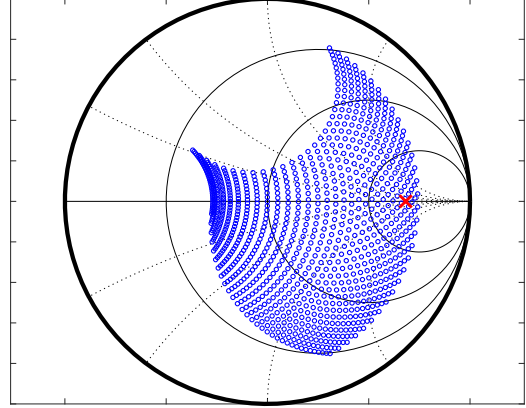


Fig. 5. Impedances matchable to $Z_{in} = 50 \Omega$. (Frequency = 27.12 MHz, $L_1 = 340 \text{ nH}$, $L_2 = 340 \text{ nH}$, $C_{01} = 140 \text{ pF}$, $C_{02} = 81 \text{ pF}$, Inductor $Q_1 = 210$, $Q_2 = 220$).

IV. A MEMS IMPEDANCE MATCHING NETWORK - EXPERIMENTAL AND MODELLED RESULTS

In order to assess the feasibility of using MEMS based switches for WPT impedance matching, a prototype printed circuit board (PCB) was designed and manufactured. A portion of the PCB is shown in Fig. 6. As mentioned previously, each variable capacitor C_{V1} , C_{V2} , is made up of six parallel branches controlled by a single MM3100 chip. An external microprocessor board (not shown) was used to control the MM3100s over their SPI interface.

Additionally, two sets of RCC resonators were designed and constructed. One pair was tuned to resonate at 13.56 MHz while the other pair was tuned for 27.12 MHz. An example set of resonators are shown in Fig. 7. Each resonator consists of two capacitive plates, two series resonant inductors, and a transformer balun. The transformer balun serves two purposes, to convert a single-ended, unbalanced signal to a balanced signal, and to perform impedance transformation.

The two resonator pairs were designed with a goal of transferring 75 W over a range of 100 mm – 200 mm. With reference to Section III, this can only be achieved with good impedance match quality if the range of load impedances, Z_L , presented to the impedance matching PCB are in the range depicted in Figs. 4, 5. For the 13.56 MHz case the impedances inherently presented by the wireless link are much larger than this range. This can be seen in Fig. 3. As such, a 2:1 balun was used on the Tx resonator to reduce the wireless link impedances by a factor of four. For the 27.12 MHz case the impedances presented by the wireless link are inherently smaller in magnitude and no impedance transformation was necessary. As a result, a 1:1 balun was used on the Tx resonator. For both frequencies, the Rx resonator was loaded with a 50 Ω impedance. A vector network analyzer (VNA) was used to measure the resonator impedances, Z_L , over the range of 100 mm – 200 mm. These values are given in Table I.

The following sections present a comparison of experimentally obtained and modelled results for impedance match quality, the node voltages on the variable capacitor



Fig. 6. MEMS-based Impedance Matching PCB

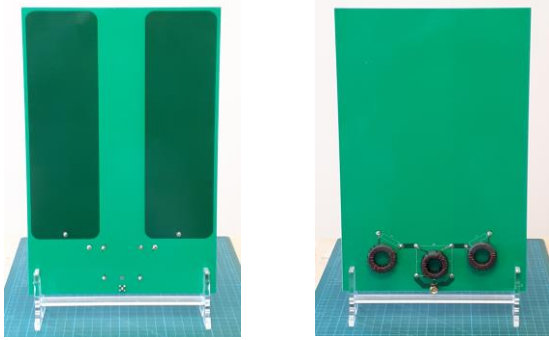


Fig. 7. Example RCC Resonator

TABLE I
RESONATOR IMPEDANCES Z_L

Resonator Displacement (mm)	Resonator Impedance 13.56 MHz (Ω)	Resonator Impedance 27.12 MHz (Ω)
100	262.40 - j7.60	258.60 + j1.04
120	161.60 - j0.33	168.53 + j1.14
140	95.75 + j0.20	98.08 + j1.82
160	58.34 - j0.25	59.13 - j0.66
180	38.20 - j0.12	38.27 - j0.26
200	27.30 - j0.10	27.68 - j0.05

branches, and the efficiency of the proposed impedance matching solution. This is carried out at both 13.56 MHz and 27.12 MHz at resonator separations of 100, 120, 140, 160, 180, and 200 mm.

A. Impedance Match Quality

The main objective of any variable impedance matching network is to convert some changing load impedance, Z_L , to match a constant source impedance of Z_0 . A laboratory power amplifier with a source impedance of 50Ω was used as the RF power source. As a result, the target impedance was $Z_0 = 50 \Omega$. For these measurements the double-L networks specified in Fig. 4 for 13.56 MHz and Fig. 5 for 27.12 MHz were used.

For each resonator displacement and corresponding load impedance given in Table 1, the best impedance matches, i.e. lowest reflection coefficient, were found. This was achieved by first positioning the resonators at the desired separation, then changing the variable capacitor branches C_{V1} , C_{V2} and measuring the resulting impedance matching input impedance, Z_{in} , on the VNA until the best match was found.

Figs. 8 and 9 show the best impedance matches obtained for the 13.56 MHz system. Both the experimental and modelled results have been plotted for comparison. Fig. 8 shows the voltage standing wave ratio (VSWR) of the impedance matching transformed impedance Z_{in} , while Fig. 9 shows the magnitude and phase of the best match. These values are plotted against the magnitude of the load impedance Z_L .

Overall the quality of the impedance matches obtained over the full operating range is quite good, with the largest VSWR being less than 1.2. However, it is important to note that in all cases the modelled results outperform the experimentally obtained results. There are several possible reasons for this. In particular, the capacitors used have component tolerances of $\pm 5\%$. As a result, the set of discrete capacitor values that can be obtained from each variable branch will not be identical to those in the model. Furthermore, each branch of the MM3100 which is turned off will have some parasitic capacitance, C_p , associated with it. The effect of this parasitic is cumulative based on the number of open switches. Finally, the PCB itself will have parasitic capacitance and inductance, as well as propagation delay due to its physical length, all of which can influence the

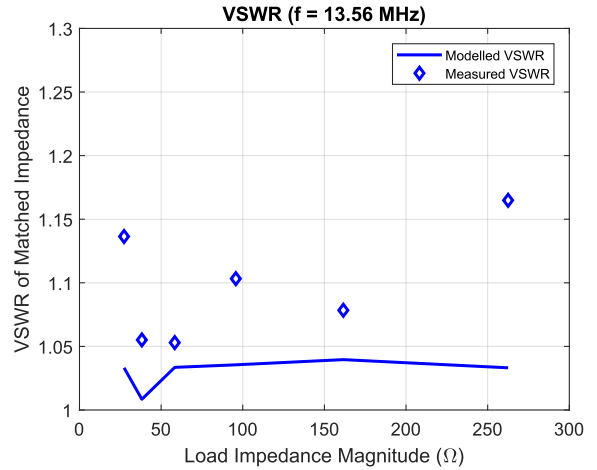


Fig. 8. VSWR of Matched Impedance for $f = 13.56$ MHz.

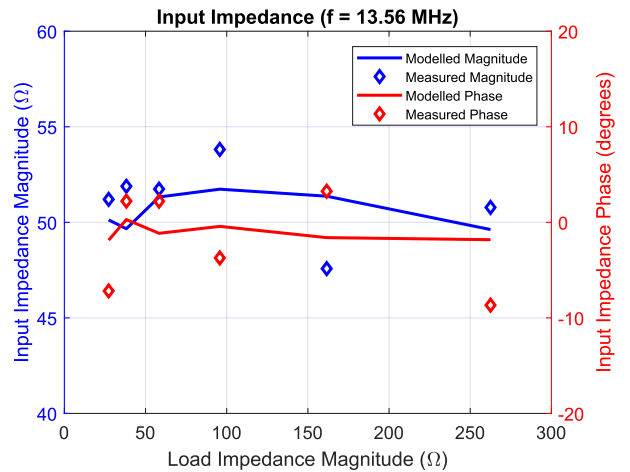


Fig. 9. Magnitude and Phase of Matched Impedance for $f = 13.56$ MHz.

final match impedance value Z_{in} . Future work would involve modelling these parasitics to improve agreement between the experimental and modelled results.

Figs. 10 and 11 show the match quality results for 27.12 MHz. Again, impedance match quality is quite good with a maximum VSWR of 1.23. However, it may be seen that the experimentally obtained best matches are not as close to the desired impedance as they were for the 13.56 MHz case. This is due to the increased influence of component and PCB parasitics at 27.12 MHz. With respect to shunt parasitic capacitance, the same capacitance at 27.12 MHz leads to a reactance which is half that of 13.56 MHz.

Most notably, the match quality drops at the closest resonator displacement of 100 mm. Here, the load impedance is $258.60 + j1.04 \Omega$ which is close to the red X shown in Fig. 5 that indicates $Z_L = 265 \Omega$. As shown in the figure, this load impedance is approaching one extreme of the matchable range. As a result, the impedance matching network has fewer

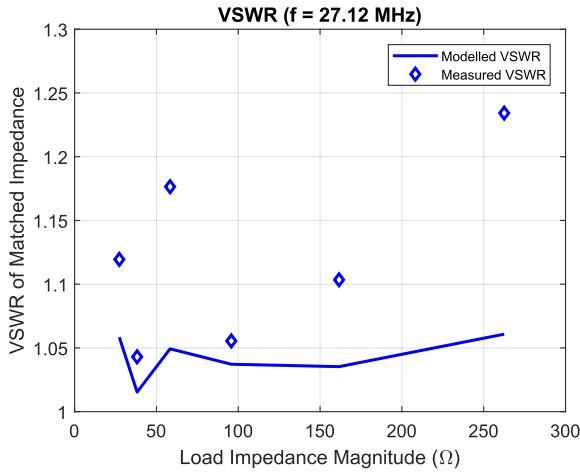


Fig. 10. VSWR of Matched Impedance for $f = 27.12$ MHz.

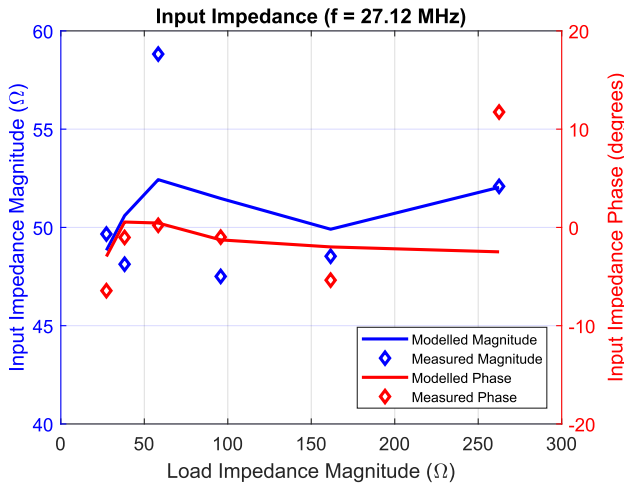


Fig. 11. Magnitude and Phase of Matched Impedance for $f = 27.12$ MHz.

available capacitor combinations to compensate for the parasitics.

B. Power Tests and Branch Voltage Measurements

In order to fully verify the use of MEMS switches for WPT impedance matching, power tests were also performed at both 13.56 MHz and 27.12 MHz. A transmit power level of 75 W into the impedance matching PCB was chosen to demonstrate the power handling abilities of the MM3100s.

For these tests, focus was placed on measuring the voltage on the two variable capacitor branches and comparing this against the modelled results. As detailed in Section III, A, it is critical to ensure the voltage on these branches stays below the maximum voltage rating of the MEMS switch. An oscilloscope was used to measure the voltage on both the C_{V1} and C_{V2} branch. The capacitance of these probes, 10 pF and 6 pF, respectively, has been included into the offset capacitance of the matching networks. For each resonator displacement the best variable capacitor combination found based on the VNA measurements was used and the input power monitored by measuring input voltage and current. The power amp RF power out was increased to approximately 75 W for each branch voltages measurement.

Fig. 12 depicts the measured and modelled branch voltages for the 13.56 MHz frequency case. The measured and modelled results are nearly identical with the only exception being the voltage on the C_{V1} branch for the load impedance of approximately 262Ω . It is important to note that this point corresponds to the match with the largest VSWR. Since the actual matched impedance deviates from the modelled matched impedance it is not surprising to see some discrepancy here.

The results for the 27.12 MHz case are shown in Fig. 13. These measurements show good agreement with the modelled results, however, there is greater deviation than that seen in the 13.56 MHz case. This is especially the case for the voltage on the C_{V1} branch. This is a direct consequence of the higher VSWR values for 27.12 MHz. Higher VSWR implies that the transformed impedance, Z_{in} , deviates more from the targeted

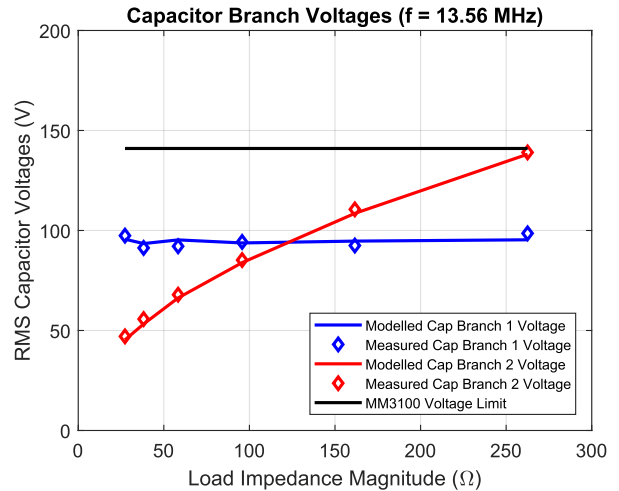


Fig. 12. RMS Branch Voltages on Variable Capacitor Branches of double-L Network for $f = 13.56$ MHz. Voltage limit of MM3100 is $V_{max} = 141 V_{rms}$.

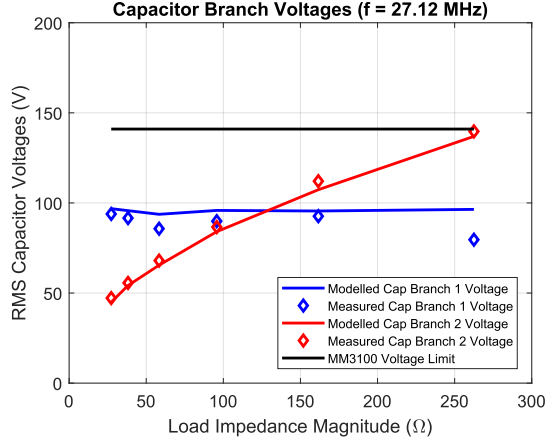


Fig. 13. RMS Branch Voltages on Variable Capacitor Branches of double-L Network for $f = 13.56$ MHz. Voltage limit of MM3100 is $V_{max} = 141$ V_{rms}.

source impedance. This can also be seen in the magnitude and phase plot for 27.12 MHz in Fig. 11. For example, the match for the largest load impedance has a fairly substantial inductive component with a phase of almost 12° . The decrease in voltage on the C_{V1} branch can be explained by this additional inductance. For the same magnitude of Z_{in} , the voltage on C_{V1} will decrease as the phase of Z_{in} increases.

The results for both frequencies show that the model is able to accurately predict the voltage stress on each variable capacitor branch. This is crucial in order to avoid an overvoltage condition which may damage the MEMS switch.

C. Impedance Matching Network Efficiency

Maximizing end-to-end efficiency of a WPT system is important for a variety of reasons, ranging from regulatory requirements to heat management. As a result, the efficiency of the proposed impedance matching solution was also measured and compared against modelled results.

The main source of loss in the double-L topology is effective series resistance (ESR) of the inductors L_1, L_2 . The loss in each inductor obviously depends on both the ESR and the current which flows through the inductor. Another source of loss is the power dissipated in the on resistance of the MEMS switch. For the MM3100 chip used in this work the on resistance is about 0.5Ω . As the voltage increases on the variable capacitor branches the current through the MEMS device increases for each variable capacitor which is switched on. Furthermore, the larger capacitance branches experience larger currents for the same branch voltage due to a lower branch reactance. Thus, the loss in the MM3100 depends on the branch voltage, the capacitance of the branch(es) which are turned on, as well as the number of branches which are turned on. The model has been developed to calculate both inductor losses as well as the loss in the MM3100s.

The efficiency of the impedance matching network was measured using a two-port VNA measurement. For each load impedance the variable capacitor branches were configured to the same values used in obtaining the best impedance match.

Figs. 14 and 15 show measured and modelled efficiency for the 13.56 MHz and 27.12 MHz cases, respectively.

The most notable trend is that the measured and modelled efficiency decreases with increasing load impedance for both frequencies. This is due to three reasons, 1) the current through inductor L_2 increases with increasing load impedance, while the current through L_1 is approximately constant, 2) the voltage on C_{V2} increases with increasing load impedance leading to higher currents through the second MM3100, and 3) the best match for larger load impedance requires more branches of the variable capacitor C_{V1} to be turned on. It may also be observed that the efficiency is lower in the 27.12 MHz case for both the modelled and measured results. This is because the inductor Q of the two double-L inductors is lower for the 27.12 MHz case (see Figs. 4, 5).

V. CONCLUSIONS

WPT impedance matching using MEMS technology has been demonstrated at a transmit power level of 75 W for operating frequencies of 13.56 MHz and 27.12 MHz. In particular, it was shown that impedance matching at this power level could be achieved over a range of 100 mm – 200 mm for RCC resonator pairs. While previous research has implemented

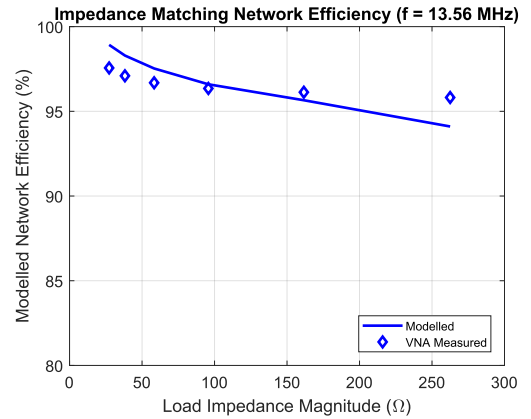


Fig. 14. RF Efficiency of double-L Matching Network for $f = 13.56$ MHz.

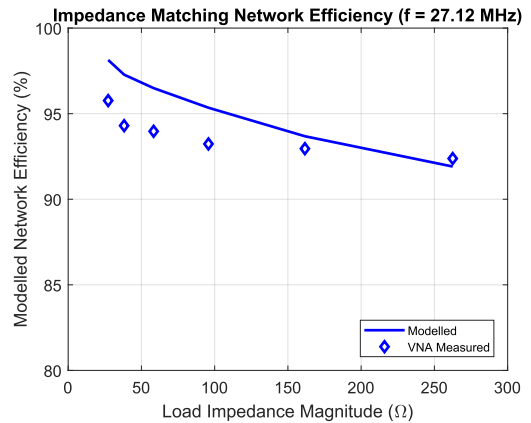


Fig. 15. RF Efficiency of double-L Matching Network for $f = 27.12$ MHz.

WPT matching, other switching methods including PIN diodes [3], varactors [4], reed relays [5], and DIP switches [1] were used. Furthermore, power levels considered in these works were 10 W and lower. Here a much higher power WPT impedance matching system based on a MEMS switch is conveyed. Moreover, this work also considers the, relatively unexplored, frequency band of 27.12 MHz. While there has been some work on WPT impedance matching at higher frequencies [4], the power levels considered were again less than 10 W.

Measurements of impedance match accuracy, MEMS device branch voltages, and RF efficiency were performed and compared against an analytical model with very good agreement. The worst-case RF efficiency of the proposed solution was 94% for the 13.56 MHz case and 92% for the 27.12 MHz system. Under optimum conditions the RF efficiency was greater than 97%. These results, coupled with the very low DC power requirements, small footprint, and minimal external biasing requirements, demonstrate the potential for MEMS based WPT impedance matching solutions.

ACKNOWLEDGMENT

This work was made possible by the generous support of the teams at Menlo Microsystems and Solace Power.

REFERENCES

- [1] A. P. Sample, B. H. Waters, S. T. Wisdom and J. R. Smith, "Enabling Seamless Wireless Power Delivery in Dynamic Environments," in *Proceedings of the IEEE*, vol. 101, no. 6, pp. 1343-1358, June 2013.
- [2] C. Keimel, G. Claydon, B. Li, J. N. Park and M. E. Valdes, "Microelectromechanical-Systems-Based Switches for Power Applications," in *IEEE Transactions on Industry Applications*, vol. 48, no. 4, pp. 1163-1169, July-Aug. 2012.
- [3] J. Bito, S. Jeong and M. M. Tentzeris, "A Real-Time Electrically Controlled Active Matching Circuit Utilizing Genetic Algorithms for Wireless Power Transfer to Biomedical Implants," in *IEEE Transactions on Microwave Theory and Techniques*, vol. 64, no. 2, pp. 365-374, Feb. 2016.
- [4] J. D. Heebl, E. M. Thomas, R. P. Penno and A. Grbic, "Comprehensive Analysis and Measurement of Frequency-Tuned and Impedance-Tuned Wireless Non-Radiative Power-Transfer Systems," in *IEEE Antennas and Propagation Magazine*, vol. 56, no. 5, pp. 131-148, Oct. 2014.
- [5] T. C. Beh, M. Kato, T. Imura, S. Oh and Y. Hori, "Automated Impedance Matching System for Robust Wireless Power Transfer via Magnetic Resonance Coupling," in *IEEE Transactions on Industrial Electronics*, vol. 60, no. 9, pp. 3689-3698, Sept. 2013.